J. Biochem. **135**, 93–99 (2004)
DOI: 10.1093/jb/mvh011

Streptomyces griseus Trypsin Is Stabilized against Autolysis by the Cooperation of a Salt Bridge and Cation-π Interaction

Weon Sup Lee, Chi Hye Park and Si Myung Byun*

Department of Biological Sciences, Korea Advanced Institute of Science and Technology, 373-1 Gusong-dong, Yusong-gu, Taejon 305-701, Korea

Received October 6, 2003; accepted November 18, 2003

***Streptomyces griseus* trypsin (SGT) is a bacterial trypsin that lacks the conserved disulphide bond surrounding the autolysis loop. We investigated the molecular mechanism by which SGT is stabilized against autolysis. The autolysis loop connects to another surface loop *via* a salt bridge (Glu146–Arg222), and the Arg222 residue also forms a cation-π interaction with Tyr217. Elimination of these bonds by site-directed mutagenesis showed that the surface salt bridge at Glu146–Arg222 is the main force stabilizing the enzyme against autolysis. The effect of the cation-π interaction at Tyr217–Arg222 is small, however, its presence increases the half-life by about five hours and enhances the protein stability more than three-fold considering the catalytic activity in the presence of the salt bridge. The melting temperature also showed cooperation between the salt bridge and cation-π interaction. These findings show that *S. griseus* trypsin is stabilized against autolysis through a cooperative network of a salt bridge and cation-π interaction, which compensate for the absence of the conserved C136–C201 disulphide bond.**

Key words: autolysis loop, cation-π interaction, cooperation, salt bridge, *S. griseus* trypsin.

Abbreviations: SGT, *Streptomyces griseus* trypsin.; L-BApNA, *N*-α-benzoyl-L-arginine-*p*-nitroanilide; Bz-L-Arg-AMC, *N*-α-benzoyl-L-arginine-7-amido-4-methyl-coumarin; Boc-Val-Pro-Arg-AMC, *t*-butyloxycarbonyl-valine-proline-arginine-7-amido-4-methyl-coumarin; Boc-Val-Leu-Lys-AMC, *t*-butyloxycarbonyl-valine-leucine-lysine-7-amido-4-methyl-coumarin; NPGB, 4-nitrophenyl-*p'*-guanidinobenzoate.

Trypsin is a chymotrypsin-like serine protease that is well conserved from bacteria to mammals in terms of both its specificity and three-dimensional structure. *S. griseus* trypsin (SGT), which has a very similar structure to mammalian trypsin, is notable for its higher catalytic activity than bovine trypsin (*1*).

The activity of dissolved trypsin decreases over time due to autolytic degradation. Throughout this article the term 'autolysis' refers to any kind of self-cleavage. The sites sensitive to autolysis are distributed in the surface loops of bovine β-trypsin, including the loop near the active site His57 (positions 59–63 in chymotrypsin numbering), the interdomain loop (positions 110–132), and the autolysis loop (positions 141–152) (*2*). Among them, the autolysis loop is the most flexible region as well as the primary target of autolytic cleavage. Studies of rat α-chymotrypsin suggest, however, that the autolysis loop may not be the structural determinant of autolytic inactivation (*3*). Also, cleavage at this site can generate fully active double chain α-trypsin in bovine β-trypsin (*4*). It has been suggested that this might be due to the C136-C201 disulphide bond that surrounds the autolysis loop, which might compensate for the effect of cleavage (*3*). The disulphide bond C136–C201 is conserved in most chymotrypsin-like proteases.

In addition to disulphide bonds, non-covalent bonds can also stabilize proteins. Since highly stable proteins from thermophilic organisms have an abundance of surface salt bridge and cation-π interactions relative to their mesophilic homologues, these electrostatic interactions are thought to be important in stabilizing protein surface loops (*5–7*). Cation-π interactions are a recently described type of non-covalent interaction between a positively charged residue and an aromatic residue (*8*). Salt bridges can form networks comprising several salt bridges (*6*). A network of salt bridges shows positive cooperation in stabilizing proteins and in enhancing the thermal stability of thermophilic proteins (*9*, *10*). Although the contribution of a single, or even several non-covalent bonds to the overall stability of the protein may be small, these bonds may be important for trapping local unfolding. Hydrogen bond networks have been reported to retard the hydrolysis of the Bowman-Birk family of serine protease inhibitors (BBIs) (*11*).

While most chymotrypsin-fold proteases have the C136-C201 disulphide bond, some, including SGT, and trypsins from *Fusarium oxysporum* and *Streptomyces erythraeus,* do not. It is interesting that all have a salt bridge between Glu146 and Arg222 (*12–14*). SGT has only one conserved autolytic sensitive site at Arg145–Glu146.

In the present work, we investigated the non-covalent bonds originating from the Glu146, and tested the effects of the elimination of those bonds by site-directed mutagenesis on the stability of SGT against autolysis.

*To whom correspondence should be addressed. Tel: +82-42-869-2612, Fax: +82-42-869-2622, E-mail: smbyun@kaist.ac.kr

Table 1. **Mutants of SGT used in this study.** Cyclic mutants were constructed to investigate the effect of amino acid changes on the catalysis and susceptibility to the proteolysis. For the salt bridge, Tyr217 was changed to Ser to eliminate the effect of cation-π interaction. For cation-π interaction, additional mutants were constructed. Mutants are named according to a combination of the single letter codes of the amino acid of residues 146, 222, and 217.

	Amino acid at position			Bond
	146	217	222	
ERY[1]	Glu	Tyr	Arg	SB[2], Cation-π
EAY	Glu	Tyr	Ala	
ARY	Ala	Tyr	Arg	Cation-π
AAY	Ala	Tyr	Ala	
ERS	Glu	Ser	Arg	SB[2]
EAS	Glu	Ser	Ala	
ARS	Ala	Ser	Arg	
AAS	Ala	Ser	Ala	

[1]wild type; [2]salt bridge.

MATERIALS AND METHODS

Materials—Bz-L-Arg-pNA, Bz-Arg-AMC, Boc-Val-Pro-Arg-AMC and Boc-Val-Leu-Lys-AMC, bovine trypsin (type I) and *p*-aminobenzamidine agarose was purchased from Sigma Chemical (St. Louis, MO). D-Val-Leu-Arg-pNA was purchased from Bachem AG (Bubendorf, Switzerland).

Cation-π Interaction Prediction in SGT—From the known structure of SGT (PDB ID: 1SGT), cation-π interactions were determined with the CaPTURE program, which predicts energetically significant cation-π interactions (*15*).

Mutant Construction—Site-directed mutagenesis of the gene encoding SGT (*16*) was performed using a Quikchange mutagenesis kit (Stratagene, La Jolla, CA, USA). Substitutions were confirmed by DNA sequencing. The structural region of the SGT gene was inserted into the *E.coli-Bacillus* shuttle vector, pSM704 (*17*), which was used to transform *B. subtilis* LB700 (*18*) by electrotransformation (*19*). The substituted amino acids and the names of the mutants are shown in Table 1. Mutants were named according to the amino acids at positions 146, 222, and 217 in order of their appearance.

Expression and Purification of the Enzymes—To date, the heterologous expression of SGT has been confined to *Streptomyces lividans* (*20*, *21*). Due to the difficulty of manipulating this host, a Bacillus expression system was constructed. Culture broth was harvested after cultivation of the transformed *Bacillus* at 30°C for 40 h, and ammonium sulfate was added to 60% saturation. After stirring for 3 h on ice, the precipitate was collected by centrifugation at 10,000 rpm, redissolved in 50 mM sodium acetate buffer (pH 5.5) containing 20 mM $CaCl_2$, filtered, and loaded onto a *p*-aminobenzamidine agarose column equilibrated with 50 mM sodium acetate buffer (pH 5.5) containing 20 mM $CaCl_2$ and 0.5 M NaCl. Bound proteins were eluted with 5 mM HCl. After dialysis in 1 mM HCl, the purified proteins were stored in 1 mM HCl at 4°C. For purification of S195A mutants, CM-sepharose chromatography on a column equilibrated with 10 mM sodium acetate (pH 5.0) was performed prior to *p*-aminobenzamidine affinity chromatography. Bound proteins were eluted with 0.2 M KCl and the eluted proteins were loaded directly onto a *p*-aminobenzamidine column. The purified enzymes were identified by immunoblotting (data not shown). All enzyme preparations were shown to be at least 95% pure by SDS/PAGE followed by Coomassie Blue staining. Active concentrations of enzyme were measured with 4-methylumbelliferyl-*p*-guanidinobenzoate (MUGB), as described previously (*22*).

SDS-PAGE—SDS-PAGE was performed as previously described (*23*). To protect against degradation during SDS-PAGE, 10 mM NPGE was added to the sample. After several minutes, the sample was diluted three fold to the buffer [10 mM Tris (pH 6.8), 1% SDS and 1% β-mercaptoethanol] before the addition of SDS-PAGE sample buffer. The sample was then heated at 75°C for five min.

Determination of Kinetic Constants—Substrate inhibition interferes with the correct determination of the k_{cat}/K_m ratio of SGT when using *N*-ester substrates, such as *N*-α-benzoyl-L-arginyl-*p*-nitroanilide (*24*). The direct determination method of the k_{cat}/K_m ratio [described on the Prolysis web site (http://delphi.phys.univ-tours.fr/Prolysis/kcat.html)] was, therefore undertaken. The assay mixture contained 100 mM NaCl, 10 mM $CaCl_2$, and 50 mM Hepes (pH 8.0), and enzyme concentrations varied from 0.5–15 nM depending on the mutant and substrates. Assays were performed using 1 ml solutions containing substrate (1.06–10.6 μM Bz-Arg-AMC, 0.1 μM Boc-Val-Pro-Arg-AMC depending on the mutant) at 25°C in an Aminco 830 spectrofluorometer. Hydrolysis of the AMC substrate was monitored fluorimetrically, with excitation at 380 nm and emission at 460 nm. The data were analyzed using Origin 6.1 software and are presented as the averages of at least two independent experiments.

Residual Activity Measurements—Enzymes (3 μM) were incubated in 50 mM Tris (pH 8.0) containing 1 mM EDTA at 30°C, and 20 μl aliquots were withdrawn at various time intervals. The residual activity of each sample was measured spectrophotometrically using BApNA (100 μM final) as a substrate in 50 mM Tris buffer (pH 8.0) containing 20 mM $CaCl_2$ at 30°C. The release of *p*-nitroaniline was monitored at 410 nm. In the case of the AAS, ARS mutant and bovine trypsin, D-Val-Leu-Arg-pNA (10 μM for AAS and ARS, 50 μM for bovine trypsin) was used as a substrate. Half-life was calculated from the equation obtained by non-linear regression analysis of the time dependence curves of residual activity (Prism 3.03, GraphPad Software). The equation utilized was $Y = Y_0\exp(kt)$, where t is the incubation time (h), Y is the relative activity (*i.e.* activity at time *t*/activity at time zero), and k is the rate constant. Half-life of inactivation was measured as $0.6932/k$. SDS-PAGE was performed to analyze the decrease in native enzymes over time. To estimate the density of the band, Gel-Pro 3.1 analyzer (Media Cybernetics) was used and the half-life was measured as mentioned above.

CD Spectroscopy—For CD measurement, the serine 195 residue of SGT (ERY) and the Y217S mutant (ERS) were changed to alanine to minimize the effect of proteolytic degradation. The samples contained 0.3 mg/ml enzyme in 10 mM Tris buffer (pH 7) or 10 mM Glycine-HCl buffer (pH 3). The protein concentration was measured using a UV-spectrophotometer as $\varepsilon^{ERY}_{280} = 23{,}045\ M^{-1}/cm$ and $\varepsilon^{ERS}_{280} = 22{,}969\ M^{-1}/cm$. The CD spectra were measured at 220 nm with a 0.1 cm path length. Changes

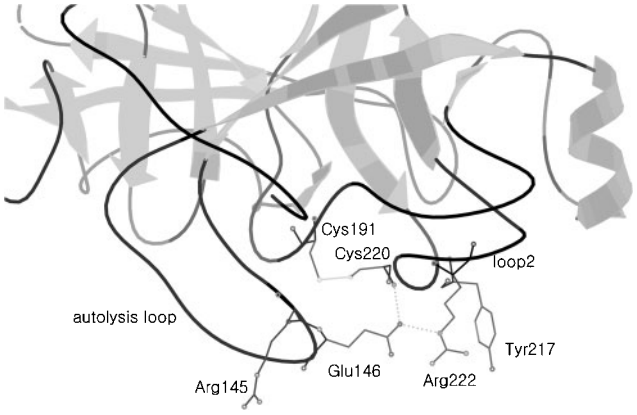

Fig. 1. **Structure surrounding the autolysis loop of SGT.** Glu146, the residue next to the autolytic sensitive site Arg145, forms a salt bridge with Arg222 located in another surface loop, loop2. The latter residue can form a cation-π interaction with Tyr217. Hydrogen bonds are also formed from Glu146OE1 to Cys220N and Arg222NE. Graph was generated using MAGE.

in ellipticity during the change in temperature from 10°C to 90°C were measured at a 0.1°C intervals. The observed CD values were normalized to the fraction of denaturation. Melting temperatures were determined using Origin 6.1 and the Boltzmann equation, $y = \{(A_1 - A_2)/(1 + e^{(x - x0)/dx}) + A_2\}$, where A_1 is the initial value, A_2 is the final value, X_0 is the midpoint (melting temperature).

RESULTS

Structure of the Autolysis Loop of SGT—Figure 1 shows the structure around the autolysis loop of SGT. The Arg145 is the only conserved autolytic sensitive site present in SGT and is the only non-bonded positively charged residue located in the surface loops of SGT (*12*). The Glu146 residue next to the autolytic sensitive Arg145 is able to form a salt bridge with Arg222 in another surface loop, called loop2, which is important for the catalytic activity of trypsin (*25*). Glu146 also forms a hydrogen bond with backbone nitrogens of Cys220 and Arg222NE. Therefore, the salt bridge Glu146–Arg222 is a hydrogen bonded salt bridge.

The CaPTURE program, which predicts energetically significant cation-π interactions, showed that Arg222 could form a cation-π interaction with Tyr217. The energy of the bond calculated by the CaPTURE program is –2.21 kcal/mol. Therefore, there is a network among Glu146, Tyr217, and Arg222 comprising a salt bridge and a cation-π interaction.

The Relative Catalytic Activity of the Enzyme Is Generally Conserved Irrespective of the Length of the Substrate—All enzymes showed similar CD spectral patterns (data not shown), suggesting that the overall structure of the mutants was not changed significantly from that of wild type SGT (ERY). Enzyme activity is closely related to the autodigestion rate. Using artificial substrates, Bz-Arg-AMC, Boc-Val-Pro-Arg-AMC, and Boc-Val-Leu-Lys-AMC, we measured the catalytic activity of all mutants (Table 2). Using Bz-Arg-AMC as a substrate, all mutants showed higher catalytic activities than bovine trypsin. The catalytic activities of the enzymes, however, differed significantly. The hydrolytic activity of ERY was about 20 times higher than that of AAS or ARS, which may result from the mutation in loop2. Mutations in loop2 are known to affect the catalytic activity of trypsin (*25*). In addition to the Tyr217 and Arg222 residues in loop2, Glu146 may also affect enzyme activity because it can form a hydrogen bond with Cys220 and a salt bridge with Arg222.

The relative enzymatic activities of the SGT variants for the hydrolysis of Bz-Arg-AMC were similar to those for Boc-Val-Pro-Arg-AMC, suggesting that the differences in activity among enzymes are maintained regardless of the length of the arginine-containing substrates. The conserved catalytic activity differences might be applied to the cleavage of the autolytic sensitive site. The relative activity was also conserved for the substrate Boc-Val-Leu-Lys-AMC, although the relative activity of the mutants to ERY was slightly lower than for the arginine containing substrates. These observations indicate that mutations of SGT at those sites can alter the catalytic power while other properties are maintained.

Autolysis of S. griseus Trypsin—Autolytic cleavage did not always lead to a collapse of the enzyme in cases when the autolyzed form was maintained by other forces, such as a disulphide bond. The cleavage of the autolysis loop of bovine trypsin containing the conserved disulphide bond

Table 2. **Catalytic activities and half-lives of enzymes.** The catalytic activities were measured for fluorogenic substrates at 25°C with excitation at 380 nm and emission at 460 nm. Note that the relative catalytic activity between enzymes was generally conserved regardless of the length of the substrate. The inactivation half-lives were measured using one-phase exponential curve fitting.

	Bz-Arg-AMC		Boc-Val-Pro-Arg-AMC		Boc-Val-Leu-Lys-AMC		Half-life (h)	Stability constant[3]
	k_{cat}/K_m[1]	Ratio[2]	k_{cat}/K_m[1]	Ratio[2]	k_{cat}/K_m[1]	Ratio[2]		
ERY	0.530	1.00	13.96	1.00	6.740	1.00	17.05 ± 0.19	17.05 ± 0.190
ERS	0.270	0.51	5.78	0.44	2.110	0.31	11.92 ± 0.11	5.25 ± 0.048
EAY	0.290	0.54	6.12	0.41	1.900	0.28	1.13 ± 0.02	0.46 ± 0.014
EAS	0.120	0.22	2.36	0.17	0.460	0.07	1.35 ± 0.01	0.23 ± 0.082
ARY	0.300	0.57	6.45	0.46	1.820	0.27	1.42 ± 0.03	0.65 ± 0.001
AAY	0.120	0.22	2.52	0.18	0.890	0.13	1.92 ± 0.04	0.35 ± 0.002
AAS	0.030	0.06	0.65	0.05	0.150	0.02	3.01 ± 0.03	0.15 ± 0.001
ARS	0.027	0.05	0.65	0.05	0.200	0.03	3.01 ± 0.02	0.15 ± 0.001
BT[4]	0.006	0.01	6.13	0.44	0.006	0.001	0.79 ± 0.01	

[1]k_{cat}/K_m value (M^{-1} s^{-1}); [2]k_{cat}/K_m value relative to wild type SGT (ERY); [3]stability constant determined by multiplying the half-life by the relative enzyme activity of the Boc-Val-Pro-Arg-AMC; [4]bovine trypsin.

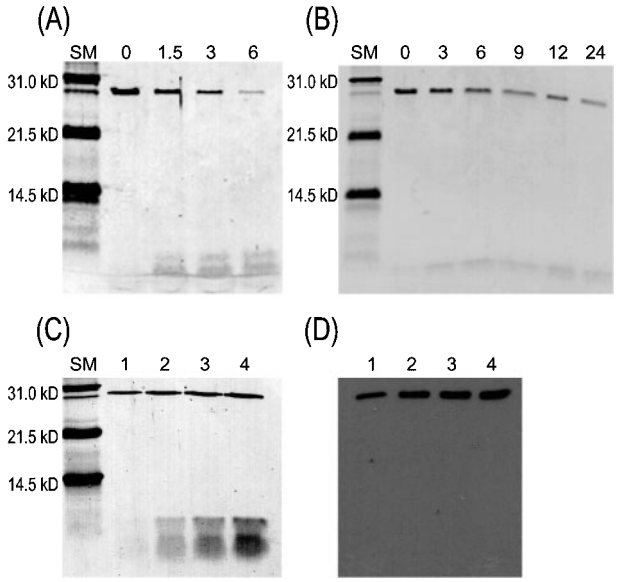

Fig. 2. **SDS-PAGE analysis of autolysis in the presence of 1 mM EDTA.** SDS-PAGE analysis of EAY (A) and ERS (B) during the time course of incubation at 30°C. The numbers above each lane indicate incubation time (h). (C), (D) SDS-PAGE analysis and western blottings of various amounts of EAY after incubation for one hour. Lane 1, 20 μl of 3 μM enzyme; 2, 20 μl of 6 μM enzyme; 3, 20 μl of 9 μM enzyme; 4, 20 μl of 12 μM enzyme. SM, molecular weight marker.

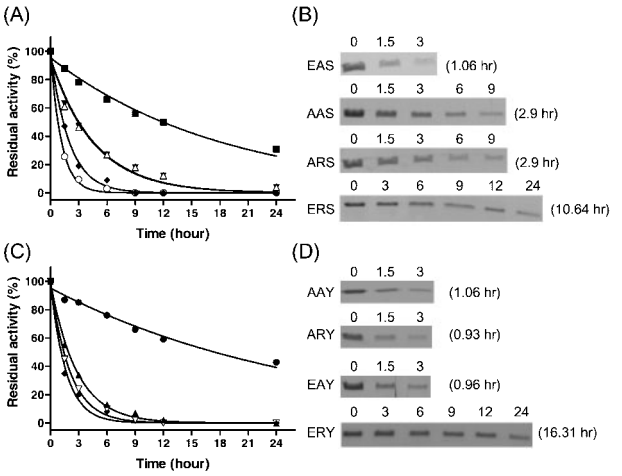

Fig. 3. **Time courses of inactivation and degradation (a), (c); Residual activities of enzymes (%) when incubated in 50 mM Tris (pH 8) containing 1 mM EDTA.** A fitted line is shown. (a) EAS (solid diamonds), AAS (inverted solid triangles), ARS (open triangles), bovine trypsin (open circles) and ERS (solid squares); (c) AAY (solid triangles), ARY (solid diamonds), EAY (inverted open triangles) and ERY (solid circles). (b), (d) ; SDS-PAGE analysis of the degradation of enzymes in (a), (c) respectively. The gels were resized for easy viewing. The densities of the bands were analyzed using a Gel-Pro 3.1 analyzer. The numbers above each lane indicate incubation time (h), numbers in parentheses are half-lives (h) of enzymes as measured by band density.

C136–C201 retains the fully active double chain form of trypsin (*4*). To investigate the patterns of autolysis of SGT, EAY, and ERS were used. EAY lacks both the salt bridge Glu146–Arg222 and the cation-π interaction Tyr217–Arg222, while ERS contains only the salt bridge. As shown in Fig. 2, a and b, no accumulated intermediate corresponding to cleavage at autolysis loop (12.8 and 15.1 kDa) could be detected irrespective of the presence of the salt bridge. This did not change when the amount of enzyme was increased (Fig. 2c). Western blot of Fig. 2c also could not detect fragments (Fig. 2d). Instead, the accumulation of degraded fragments was shown. This suggests that the force holding the cleaved structure of SGT is very small irrespective of the presence of the salt bridge. Also, the half-life as determined by activity and gel-band density was generally similar (Table 2, Fig. 3). This implies that the autolyzed form of SGT was maintained briefly and degraded further just after autolysis. The higher catalytic activity of SGT may also contribute to the short retention of the cleaved form. SGT (210 residues) was migrated as a 28 kDa protein on SDS-PAGE. Although the reason this behavior on SDS-PAGE is not known, trypsin (230 residues) from *Streptomyces erythraeus* (SET) also shows this anomalous behavior, migrating as a 35 kDa protein on SDS-PAGE (*20*).

The Glu146–Arg222 Salt Bridge Stabilize S. griseus Trypsin Against Autolysis—The rate of autolysis by members of the trypsin family has long been known to depend on calcium concentration. As expected, calcium stabilized SGT variants and the difference in the stability against autolysis was small (data not shown). To maximize the differences between SGT variants, EDTA was added in our assay. To investigate the effect of non-covalent bonds on autolysis, cyclic mutants were constructed (Table 1). For the salt bridge, all mutants had serine as the 217th residue instead of tyrosine to remove the effect of the cation-π interaction. Figure 3 shows the time-courses for the decreasing activity and band density of the mutants. The inactivation fits a one-phase exponential curve, and is a first order reaction. The half-lives as determined by inactivation and band density were generally similar, although the latter were shorter than the former. This also indicates that the retention time of the autolyzed enzyme is very short, and the half-life is closely related to the susceptibility of the autolysis loop. ERS had an inactivation half-life of 11.92 h, while most of the mutants lacking the salt bridge had half-lives of about 1.1–1.9 h, except AAS and ARS, which had half-lives of 3.01 h (Table 2 and Fig.3). The relatively slower inactivation of AAS and ARS resulted from their lower catalytic activities in comparison to other mutants. In addition, the relative catalytic activity was generally conserved among all mutants as shown in Table 2. A similar situation was also shown for the half-life of AAY, which also showed lower catalytic activity. Therefore, we considered relative catalytic activity in normalizing the half-lives of the enzymes. This is the stability constant. In comparing the stability constants of EAS and AAS, the mutant containing Glu at the P1′ residue showed stability similar to the mutant containing Ala at P1′. This indicates that changes at the P1′ residue do not affect the susceptibility of the autolysis loop. This tendency was also shown in comparing the stabilities of EAY and AAY. As with the Glu/Ala change at position 146, the Arg/Ala at position 222 did not affect the stability because the stability constants of ARS and AAS are similar. Therefore, the difference in stability between ERS and ARS is the result of

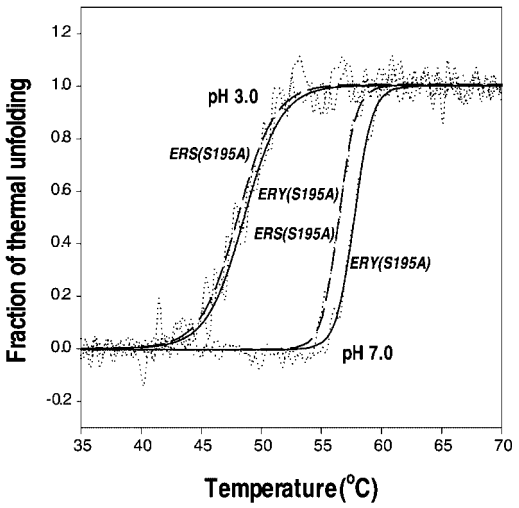

Fig. 4. **Melting temperatures (T_m) of ERY (S195A) and ERS (S195A).** The thermal unfolding at two pH values were determined by circular dichroism at 220 nm. Dotted lines indicate thermal unfolding of the proteins. Dashed lines indicate the fitted line of ERS (S195A). Straight lines indicate the fitted line of ERY (S195A). T_m of ERY (S195A) was 57.739 ± 0.0323 °C at pH 7 and 48.583 ± 0.174 °C at pH 3. T_m of ERS (S195A) was 56.472 ± 0.0321 °C at pH 7 and 48.068 ± 0.172 °C at pH 3.

the presence of a salt bridge. ERS is about 35 times more stable than ARS based on their activity difference. It can be concluded that the salt bridge at Glu146–Arg222 stabilizes the enzyme to autolysis. All mutants inactivated more slowly than bovine trypsin (0.76 h), although it was not possible to compare the SGT variants directly because catalytic activity of bovine trypsin is significantly different as to substrates and it has three autolysis sensitive sites.

A Cation-π Interaction Contributes to the Stability of S. griseus Trypsin—Figure 3, b and d, shows the time-course of decreasing activity and enzyme band density (ERY, AAY, ARY, and EAY), respectively. The effect of Tyr/Ser217 on the stability was also small (compare the stability constants of EAY/EAS and AAY/AAS). The cation-π interaction slightly stabilizes the enzyme, but the effect is relatively small compared to the salt bridge because the stability constant of ARY is only 12 percent that of ERS. This indicates that the main force stabilizing the autolysis loop is the Glu146–Arg222 salt bridge as expected. The effect of the cation-π interaction is enhanced when it is connected to the Glu146–Arg222 salt bridge. ERY, an enzyme containing both the salt bridge and cation-π interaction, had a half-life five hours longer than that of ERS despite, its higher catalytic activity. The stability constant of ERY is 325 percent higher than that of ERS. These results indicate that a non-covalent bond network formed by a salt bridge and cation-π interaction can cooperate in stabilizing proteins against autolysis.

Cooperation of the Salt Bridge and Cation-π Interaction as Measured by Melting Temperature—As another approach to show the cooperation of the network formed by a salt bridge and cation-π interaction, the melting temperatures of ERY(S195A) and ERS(S195A) were measured at two pH values, pH 7 and pH 3. While the salt bridge forms at pH 7, would be broken or weakened at pH 3, while the cation-π interaction would be present at both pH values. At each pH value, a difference in melting temperature between the two enzymes might result from the presence of the cation-π interaction and the different amino acid at position 217 (Tyr/Ser). Using the difference in melting temperature at these two pH values, the effect of the amino acid difference on the melting temperature would be removed. Thus, if there is cooperation between the two bonds, the difference in melting temperature will be larger at pH 7 than at pH 3. The thermal denaturation was reversible at pH 3, but not at pH 7 (data not shown). As the temperature was elevated, a precipitate was formed at pH 7. We found that the melting temperature of ERY (S195A) was 57.739 ± 0.0323°C at pH 7 and 48.583 ± 0.174°C at pH 3, while the melting temperature of ERS (S195A) was 56.472 ± 0.0321°C at pH 7 and 48.068 ± 0.172°C at pH 3 (Fig. 4). Since the difference in melting temperature was larger at pH 7 (1.18°C) than at pH 3 (0.53°C), our results indicate that there is cooperation between the salt bridge (Glu146–Arg222) and cation-π interaction (Tyr217–Arg222). While the difference is small, however, it could be important in the local unfolding of the site susceptible to proteolysis.

DISCUSSION

We have shown here that SGT is stabilized against autolysis by the cooperation of a salt bridge and a cation-π interaction. This is the first report of this type of cooperation. Although the contribution of several non-covalent bonds to the overall stability of SGT may be small, as shown in Figure 4, these bonds can contribute to trapping local unfolding of the some regions on the protein. Recent modeling studies of a number of proteolytic sites in various proteins indicate that preferential cleavage site recognition may be controlled by local unfolding and structural adaptation of the enzyme active site (*26*). The Glu146–Arg222 salt bridge, located next to the autolysis sensitive Arg145, can decrease the local unfolding of the autolysis loop and lower the rate of cleavage. As shown in Fig. 4, the difference in thermal stability between ERY(S195A) and ERS(S195A) is small, but such small differences can have a significant effect in protecting proteins from proteolysis, because they can retard the local unfolding of the susceptible site.

We introduced the stability constant to normalize the half-life. The hydrolysis of Boc-Val-Pro-Arg-AMC was used to determine relative catalytic activity, but the results were not changed significantly if Boc-Arg-AMC was used instead. The correlation between the activity to hydrolyze an artificial substrate and the activity to hydrolyze a protein substrate was inferred from the results that 1) the relative catalytic activity of the enzyme was conserved as the length of the substrate grew longer and 2) the cleavage rate of mutants lacking the both non-covalent bonds (EAS, EAY, AAS, AAY, and ARS), as shown in Fig. 3, b and d, was generally correlated to the relative catalytic activity.

The kinetics of autolysis found in this study fit well to a single-phase exponential equation as shown in Fig. 3. SGT might be degraded just after proteolytic cleavage at the autolysis loop because no intermediate corresponding to the autolyzed form could be detected as shown in Fig.

2, and the half-lives determined by activity and gel band density were similar (Fig. 3). This might be the cause for the apparent first order kinetics of SGT. The kinetics of autolysis about the chymotrypsin was also apparently first order when higher enzyme concentrations were used (*ca.* 2–27 mg/ml), while apparent second order kinetic were found when lower enzyme concentrations were used (1 mg/ml) (*27*). This can be also explained by the fact that the retention time of the autolyzed enzyme would be relatively short under conditions of higher enzyme concentration than lower enzyme condition. At higher concentrations, chymotrypsin would be degraded just after autolysis as in the case of SGT.

The Glu146–Arg222 salt bridge is also present in other serine proteases, including trypsins from *S. erythraeus* (bacteria) (*14*) and *F. oxysporum* (Fungi) (*13*) and human α-thrombin (mammal) (*28*). All lack the disulphide bond surrounding the autolysis loop. These findings suggest that the salt bridge formed during the evolution of serine proteases that lack the C136–C201 disulphide bond to stabilize them against autolysis. Although the contribution of the disulphide bond to the overall stability (up to 4 kcal/mol) (*29*, *30*) is generally larger than that of the surface salt bridge (0.1 to 0.5 kcal/mol) (*31*), it is hard to compare their effects directly because they each stabilize the molecule against autolysis in a different manners. The salt bridge may guard against local unfolding of the autolytic sensitive site (Arg145), whereas the C136–C201 disulfide bond likely retards autolysis by stabilizing the molecule against systemic unfolding, as is its purpose in many other chymotrypsin-like proteases. Additionally, in the case of SGT, the contribution of the salt bridge is increased by networked cation-π interactions. It has been reported that the absence of disulphide bonds results in increased protein yield (*32*). Thus, the introduction of a non-covalent bond network into SGT may be an efficient way to confer stability against autolysis and to increase the protein yield.

Cooperation between non-covalent bonds has been studied extensively in salt bridge networks. Of special interest is the contribution of these bonds to the thermal stability of proteins from thermophiles (*10*). In this study, we show that a salt bridge and cation-π interaction are able to form a cooperative network. It has been reported that cation-π interactions are stronger than salt bridges in aqueous environments, but the situation is reversed in hydrophobic environments (*33*), suggesting that the replacement of a surface salt bridge with a cation-π interaction in a network of electrostatic interactions may enhance protein stability.

Authors thank Dr. Kyoung-Seok Ryu (Korea Advanced Institute of Science and Technology) and Dr. Key-Sun Kim (Korea Institute of Science and Technology) for helpful discussions.

REFERENCES

1. Hatanaka, Y., Tsunematsu, H., Mizusaki, K., and Makisumi, S. (1985) Interactions of derivatives of guanidinophenylalanine and guanidinophenylglycine with *Streptomyces griseus* trypsin. *Biochim. Biophys. Acta* **832**, 274–279
2. Maroux, S. and Desnuelle, P. (1969) On some autolyzed derivatives of bovine trypsin. *Biochim. Biophys. Acta* **181**, 59–72
3. Bodi, A., Kaslik, G., Venekei, I., and Graf, L. (2001) Structural determinants of the half-life and cleavage site preference in the autolytic inactivation of chymotrypsin. *Eur. J. Biochem.* **268**, 6238–6246
4. Walsh, K.A. (1970) Trypsinogens and trypsins of various species. *Methods Enzymol.* **19**, 41–64
5. Hennig, M., Darimont, B., Sterner, R., Kirschner, K., and Jansonius, J.N. (1995) 2.0 A structure of indole-3-glycerol phosphate synthase from the hyperthermophile *Sulfolobus solfataricus*: possible determinants of protein stability. *Structure* **3**, 1295–1306
6. Yip, K.S., Stillman, T.J., Britton, K.L., Artymiuk, P.J., Baker, P.J., Sedelnikova, S.E., Engel, P.C., Pasquo, A., Chiaraluce, R., and Consalvi, V. (1995) The structure of *Pyrococcus furiosus* glutamate dehydrogenase reveals a key role for ion-pair networks in maintaining enzyme stability at extreme temperatures. *Structure* **3**, 1147–1158
7. Luisi, D.L., Snow, C.D., Lin, J.J., Hendsch, Z.S., Tidor, B., and Raleigh, D.P. (2003) Surface salt bridges, double-mutant cycles, and protein stability: an experimental and computational analysis of the interaction of the Asp 23 side chain with the N-terminus of the N-terminal domain of the ribosomal protein L9. *Biochemistry* **42**, 7050–7060
8. Dougherty, D.A. (1996) Cation-pi interactions in chemistry and biology: a new view of benzene, Phe, Tyr, and Trp. *Science* **271**, 163–168
9. Albeck, S., Unger, R., and Schreiber, G. (2000) Evaluation of direct and cooperative contributions towards the strength of buried hydrogen bonds and salt bridges. *J. Mol. Biol.* **298**, 503–520
10. Kumar, S. and Nussinov, R. (2002) Close-range electrostatic interactions in proteins. *Chembiochem.* **3**, 604–617
11. McBride, J.D., Brauer, A.B., Nievo, M., and Leatherbarrow, R.J. (1998) The role of threonine in the P2 position of Bowman-Birk proteinase inhibitors: studies on P2 variation in cyclic peptides encompassing the reactive site loop. *J. Mol. Biol.* **282**, 447–458
12. Read, R.J. and James, M.N. (1988) Refined crystal structure of *Streptomyces griseus* trypsin at 1.7 Å resolution. *J. Mol. Biol.* **200**, 523–551
13. Rypniewski, W.R. (1995) Structure of inhibited trypsin from *Fusarium oxysporum* at 1.55 A. *Acta Crystallogrphica Section D* **54**, 73–84
14. Yamane, T., Iwasaki, A., Suzuki, A., Ashida, T., and Kawata, Y. (1995) Crystal structure of Streptomyces erythraeus trypsin at 1.9 A resolution. *J. Biochem.* **118**, 882–894
15. Gallivan, J.P. and Dougherty, D.A. (1999) Cation-pi interactions in structural biology. *Proc. Natl Acad. Sci. USA* **96**, 9459–9464
16. Kim, J.C., Cha, S.H., Jeong, S.T., Oh, S.K., and Byun, S.M. (1991) Molecular cloning and nucleotide sequence of *Streptomyces griseus* trypsin gene. *Biochem. Biophys. Res. Commun.* **181**, 707–713
17. Bae, K.H., Kim, I.C., Kim, K.S., Shin, Y.C., and Byun, S.M. (1998) The Leu-3 residue of *Serratia marcescens* metalloprotease inhibitor is important in inhibitory activity and binding with *Serratia marcescens* metalloprotease. *Arch. Biochem. Biophys.* **352**, 37–43
18. Lee, S.J., Kim, D.M., Bae, K.H., Byun, S.M., and Chung, J.H. (2000) Enhancement of secretion and extracellular stability of staphylokinase in *Bacillus subtilis* by *wprA* gene disruption. *Appl. Environ. Microbiol.* **66**, 476–480
19. Matsuno Y., T.A., and M., Shoda (1992) High-efficiency transformation of *Bacillus subtilis* NB22, an antifungal antibiotic iturin producer, by electroporation. *J. Ferment. Bioeng.* **73**, 261
20. Nagamine-Natsuka, Y., Norioka, S., and Sakiyama, F. (1995) Molecular cloning, nucleotide sequence, and expression of the gene encoding a trypsin-like protease from *Streptomyces erythraeus*. *J. Biochem.* **118**, 338–346
21. Koo, B.J., Bae, K.H., Byun, S.M., and Hong, S.K. (1998) Purification and characterization of *Streptomyces griseus* trypsin

overexpressed in *Streptomyces lividans*. *J. Microbiol. Biotechnol.* **8**, 333–340
22. Coleman, P.L., Lathham, H.G., Jr., and Shaw, E.N. (1976) Some sensitive methods for the assay of trypsinlike enzymes. *Methods Enzymol.* **45**, 12–26
23. Yokosawa, H., Hanba, T., and Ishii, S. (1976) Affinity chromatography of trypsin and related enzymes. III. Purification of *Streptomyces griseus* trypsin using an affinity adsorbent containing a tryptic digest of protamine as a ligand. *J. Biochem.* **79**, 757–763
24. Nakata, H., Yoshida, N., Narahashi, Y., and Ishii, S. (1972) Substrate activation and substrate inhibition of trypsin-like enzymes from three strains of *Streptomyces species*. *J. Biochem.* **71**, 1085–1088
25. Hedstrom, L., Szilagyi, L., and Rutter, W.J. (1992) Converting trypsin to chymotrypsin: the role of surface loops. *Science* **255**, 1249–1253
26. Hubbard, S.J., Beynon, R.J., and Thornton, J.M. (1998) Assessment of conformational parameters as predictors of limited proteolytic sites in native protein structures. *Protein Eng.* **11**, 349–359
27. Kumar, S. and Hein, G.E. (1970) Concerning the mechanism of autolysis of alpha-chymotyrpsin. *Biochemistry* **9**, 291–297
28. Rydel, T.J., Ravichandran, K.G., Tulinsky, A., Bode, W., Huber, R., Roitsch, C., and Fenton, J.W., 2nd. (1990) The structure of a complex of recombinant hirudin and human alpha-thrombin. *Science* **249**, 277–280
29. Shaw, A. and Bott, R. (1996) Engineering enzymes for stability. *Curr. Opin. Struct. Biol.* **6**, 546–550
30. Clarke, J. and Fersht, A.R. (1993) Engineered disulfide bonds as probes of the folding pathway of barnase: increasing the stability of proteins against the rate of denaturation. *Biochemistry* **32**, 4322–4329
31. Sali, D., Bycroft, M., and Fersht, A.R. (1991) Surface electrostatic interactions contribute little of stability of barnase. *J. Mol. Biol.* **220**, 779–788
32. Vindigni, A. and Di Cera, E. (1998) Role of P225 and the C136-C201 disulfide bond in tissue plasminogen activator. *Protein Sci.* **7**, 1728–1737
33. Gallivan, J.P. and Dougherty, D.A. (2000) A computational study of cation-pi interactions vs salt bridgesin aqueous media: Implications for protein engineering. *J. Amer. Chem. Soc.* **122**, 870–874